

## Fluid dynamical effects of polymers adsorbed to spherical particles

John L. Anderson and JeonOk Kim

Citation: [The Journal of Chemical Physics](#) **86**, 5163 (1987); doi: 10.1063/1.452637

View online: <http://dx.doi.org/10.1063/1.452637>

View Table of Contents: <http://scitation.aip.org/content/aip/journal/jcp/86/9?ver=pdfcov>

Published by the [AIP Publishing](#)

---

### Articles you may be interested in

[Solvation force induced by short range, exact dissipative particle dynamics effective surfaces on a simple fluid and on polymer brushes](#)

J. Chem. Phys. **134**, 014703 (2011); 10.1063/1.3517869

[The Effects of a Constant Bias Force on the Dynamics of a Periodically Forced Spherical Particle in a Newtonian Fluid at Low Reynolds Numbers](#)

AIP Conf. Proc. **1281**, 43 (2010); 10.1063/1.3498501

[Wall Effects on a Single Spherical Particle Moving Through a Carreau Model Fluid](#)

AIP Conf. Proc. **1152**, 110 (2009); 10.1063/1.3203259

[Nucleation in binary polymer blends: Effects of foreign mesoscopic spherical particles](#)

J. Chem. Phys. **121**, 1105 (2004); 10.1063/1.1761053

[Statistical thermodynamics of a fluid adsorbed onto a spherical surface. II. Scaled particle theory](#)

J. Chem. Phys. **88**, 5805 (1988); 10.1063/1.454539

---



# Fluid dynamical effects of polymers adsorbed to spherical particles

John L. Anderson and Jeen-Ok Kim

Department of Chemical Engineering, Carnegie Mellon University, Pittsburgh, Pennsylvania 15213

(Received 30 September 1986; accepted 27 January 1987)

The effects of adsorbed macromolecules (polymers) on certain transport coefficients of spherical particles are determined using methods of matched asymptotic expansions to solve the Stokes flow equations within and outside the polymer layer. The main advantage of this analysis is that it allows direct substitution of a linear, viscous model for flow through the polymer segments to obtain the desired transport coefficient without solving the entire set of fluid dynamics equations. The results, expressed as an effective "hydrodynamic thickness" ( $L_h$ ) of the adsorbed polymer, are accurate to  $O(\lambda)$  where  $\lambda$  is the ratio of the polymer-layer length scale to the particle radius. Three flow configurations are considered: steady translation and steady rotation of a single particle, and pure straining flow around a single particle that produces stresses leading to enhanced viscosity of a suspension (intrinsic viscosity). The Reynolds number is assumed to be small in all cases. The  $O(\lambda^0)$  term for  $L_h$  is the same for all three flows, but the  $O(\lambda)$  corrections differ. Sample calculations show that (1) the  $O(\lambda)$  correction is negative, meaning  $L_h$  increases as particle radius increases assuming all other conditions are constant; (2) a free-draining model for flow through the polymer chains is a very good approximation for calculating  $L_h$  if the Stokes radius of the polymer segments is much smaller than the length scale of the polymer scale; and (3) the presence of only a small amount of adsorbed polymer "tails" can make a significant contribution to  $L_h$  if the length scale of the extended tails exceeds the length scale of the "loops" by a factor of 2 or more. Finally, we derive the hydrodynamic response of a particle having polymer *nonuniformly* adsorbed to its surface and demonstrate through a sample calculation how an "adsorption dipole" can lead to strong orientational bias of the particle as it moves in response to an applied force.

## INTRODUCTION

Adsorption of macromolecules to a fluid/solid interface causes changes in viscous interactions between the fluid and solid phases. For example, adsorption of proteins<sup>1</sup> or linear polymers<sup>2</sup> to a porous membrane reduces the hydraulic permeability of the membrane, while the diffusion coefficient of colloidal particles is reduced when polymers are adsorbed to their surfaces.<sup>3,4</sup> The changes in these transport parameters are in directions indicating a greater friction between the fluid and solid phases and these results are often interpreted in terms of a change in dimension of the pores or particles, which is called the "hydrodynamic thickness" ( $L_h$ ) of the adsorbed polymer layer. Of course there is no unique measure of the layer thickness due to the diffuseness of the polymer chains; thus, while  $L_h$  is certainly correlated with the length scale characterizing extension of the chains from the interface, it is still just an experimentally defined parameter rather than a true physical length.

There are three basic problems associated with modeling the effect of adsorbed polymers on the hydrodynamic response of particles. First, a model for configuration of the adsorbed polymer is required; second, a local rheological model for flow through the polymer layer must be developed; and third, the fluid dynamical equations must be solved both within and outside the polymer layer to determine the fluid stresses on a particle and then obtain the desired transport parameter. The focus of this paper is on the third problem; the objective is to place the fluid dynamical description in a sufficiently simple form that allows models

of polymer configuration and rheology to be inserted for direct computation of  $L_h$ .

Theoretical work by Hoeve,<sup>5,6</sup> Silberberg,<sup>7,8</sup> and deGennes<sup>9,10</sup> on adsorption of polymers to flat interfaces assumes two types of structures, "trains" which are attached to the interface and "loops" which extend into the fluid and experience restricted Brownian movement. Their work established that the density of polymer segments in the loops decays exponentially with distance from the interface:

$$\rho = \rho_0 e^{-y}, \quad (1)$$

where  $y$  is the distance normalized by a length scale ( $\delta$ ) which depends on the molecular weight of the polymer, the amount of polymer adsorbed and the relative interactions among the polymer, interface, and fluid. For example, for a given amount of polymer adsorbed an improvement in the goodness of the solvent will cause expansion of the loops and thus an increase in  $\delta$ .

More recent theories based on lattice statistics<sup>11-14</sup> show a significant number of "tails", which are the ends of polymer molecules that are attached to trains. The important aspect of the tails from our point of view is that the length scale of their segment distribution is substantially greater, by a factor of 4 in some cases,<sup>13</sup> than for the loops. It is clear from several studies<sup>4,15</sup> that in general the hydrodynamic effects of the tails cannot be ignored.

There is little theory available for the local rheology within adsorbed polymer layers. Presently acceptable models consist of a Darcy-law-type model with the permeability coefficient being an explicit function of the local polymer

segment density. The force density produced by Stokes friction between polymer segments and the fluid is of the form

$$-\xi \rho f(\mathbf{v} - \mathbf{v}^{(p)}),$$

where  $\xi$  is the friction coefficient of an isolated polymer segment ("bead"),  $\mathbf{v}$  is the fluid velocity, and  $\mathbf{v}^{(p)}$  is the velocity of the segments at the position in question, and  $f$  is a function of  $\rho$  which accounts for hydrodynamic interactions among segments. For a free-draining hydrodynamic model  $f = 1$ , while segment-segment interactions cause  $f$  to increase with  $\rho$ . If the polymer segments are modeled as rigid spheres with radius  $a$  equal to the Stokes radius,

$$a = \frac{\xi}{6\pi\mu_s}, \quad (2)$$

then  $f$  is given by a Brinkman-type expression<sup>16</sup> at low  $\rho$  and by an expression such as the Blake-Kozeny equation<sup>17</sup> at high  $\rho$ . One should note that these equations were derived assuming  $\rho$  is uniform, whereas  $\rho$  is an exponentially decaying function of distance from the interface in an adsorbed polymer layer.

Based on the above discussion, we choose to model the fluid dynamics of flow about a particle with adsorbed polymer on its surface by the Stokes equations modified to account for the force density ( $\beta$ ) and viscous effects ( $\mu$ ) of the polymer segments:

$$\nabla \cdot [\mu(\nabla \mathbf{v} + \nabla \mathbf{v}^T)] - \nabla p - \lambda^{-2} \beta(\mathbf{v} - \mathbf{v}^{(p)}) = 0, \quad (3a)$$

$$\nabla \cdot \mathbf{v} = 0. \quad (3b)$$

Dimensionless variables are used, with  $\mathbf{v}$  and  $\mathbf{v}^{(p)}$  normalized by a characteristic velocity ( $V^*$ ),  $\mu$  by the solvent viscosity ( $\mu_s$ ),  $\nabla$  by the particle radius ( $R$ ), and  $p$  by  $\mu_s V^*/R$ . The dimensionless parameter  $\beta$  is defined as

$$\beta = \frac{\delta^2 \xi}{\mu_s} \rho f \quad (4)$$

and is  $O(1)$  with respect to  $\lambda$  which equals the ratio  $\delta/R$  and is assumed to be small. Note that if Eq. (1) describes the segment distribution at  $y \gg 1$  then both  $\beta$  and  $(\mu - 1)$  decay to zero exponentially with  $y$ , and hence the hydrodynamic effect of the polymer is localized to a thin layer near the particle's surface. Previous theories of flow in adsorbed polymer layers have assumed  $\mu = 1$ ; here, we allow  $\mu$  to be a function of  $\rho$ , although calculations discussed later show that effects of  $\mu > 1$  are negligible compared to the effects of  $\beta$ .

Given Eq. (3) and an expression for  $\rho(y)$ , the task is to solve for  $\mathbf{v}$  and then compute the fluid forces on the interface. Analyses found in the literature are restricted to one-dimensional flows past a stationary interface. Thus, with the exception of the work by Varoqui and Dejaridin<sup>18</sup> on the theory of pressure-driven flow through long pores with polymer adsorbed to the wall, the results of the current literature are valid only for the limit  $\lambda \rightarrow 0$ . Furthermore, these hydrodynamic calculations for flat interfaces have been applied in an *ad hoc* manner in order to compute the hydrodynamic thickness of polymer adsorbed to spherical particles. There is currently lacking a general fluid dynamical analysis, based on Eq. (3), which can be used to evaluate or interpret experimental data for particles in various flow configurations. Our

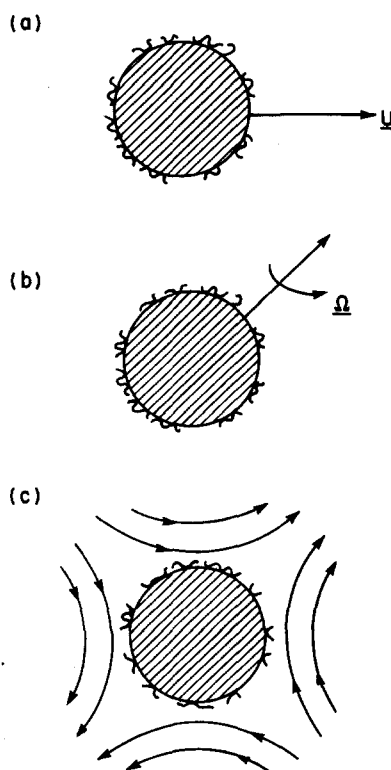


FIG. 1. Flow configurations: (a) translation, (b) rotation, and (c) pure straining flow.

objective here is to develop such an analysis and demonstrate its usefulness through examples.

We consider a single spherical particle which could be in one of the three flow configurations shown in Fig. 1.  $L_h$  is defined as the increase in particle radius needed to account for the measurable effect of the adsorbed polymer on the particle-fluid interaction in each flow. In all cases Eq. (3) describes the fluid dynamics and  $\rho(y)$  is assumed to be independent of  $\lambda$ ; the latter assumption is relaxed in the Discussion section. The analysis is general for any  $\rho(y)$  that decays to zero at large  $y$  faster than  $y^{-4}$ . Both loops and tails, or even a mixture of polymers having different adsorbed length scales ( $\delta$ ) can be included in the model.

Our approach is to solve Eq. (3) within and outside the polymer layer using expansions in  $\lambda$  and then match these expansions at the outer edge of the polymer layer. After computing the relevant fluid stresses on the particle, we obtain an expression for the hydrodynamic thickness having the form

$$L_h = A\delta[1 + B\lambda], \quad (5)$$

which has an error of  $O(\lambda^2)$ . In the next section we go through the details of the analysis assuming a uniform coverage of a particle's surface by the polymer. The result for  $A$  is the same for all three flow configurations and is found in Eqs. (22) and (24a), while  $B$  is given by Eqs. (23) and (24b), Eqs. (34) and (35b), or Eqs. (46) and (48b) for translation, rotation, or intrinsic viscosity.  $A$  and  $B$  are evaluated for different physical conditions to probe the effects of hydrodynamic interactions among the polymer segments

and the contributions to  $L_h$  made by adsorbed tails vs loops. We then focus our attention on the limit  $\lambda \rightarrow 0$  and argue that the hydrodynamic effect of an adsorbed polymer is fundamentally due to a "slip velocity" that appears to exist at the outer edge of the adsorbed layer. Using this concept we develop expressions [Eq. (57)] for the force and torque on a translating, rotating particle that may have a *nonuniform* coverage of polymer on its surface. An example indicates that a small dipole moment of the polymer coverage can result in strong alignment of a particle undergoing sedimentation.

## II. ANALYSIS OF FLOW AROUND A PARTICLE HAVING POLYMER UNIFORMLY ADSORBED TO ITS SURFACE

### A. Translation of a particle

In the absence of adsorbed polymer, the frictional force on a particle moving at velocity  $\mathbf{U}$  is given by Stokes law:

$$\mathbf{F}_f^{(0)} = -6\pi\mu_s R \mathbf{U} \quad (\text{no polymer}). \quad (6)$$

After adsorption of polymer the frictional force increases. The hydrodynamic thickness of the polymer layer is defined as the increase in size of the particle needed to account for this extra drag:

$$\mathbf{F}_f = -6\pi\mu_s (R + L_h) \mathbf{U} \quad (\text{adsorbed polymer}). \quad (7)$$

The problem is to compute  $\mathbf{F}_f$  by solving the modified Stokes equations and then use Eq. (7) to determine  $L_h$ .

The coordinate system is centered on and moves with the particle; in this moving coordinate system  $\mathbf{v}^{(p)} = 0$ . Equation (3) must be solved subject to the following boundary conditions:

$$r = 1: \quad \mathbf{v} = 0, \quad (8a)$$

$$r \rightarrow \infty: \quad \mathbf{v} \rightarrow -\mathbf{k}. \quad (8b)$$

$\mathbf{k}$  is the unit vector aligned with the direction of  $\mathbf{U}$ , and  $(r, \theta, \phi)$  is the standard spherical-coordinate system. The solution for  $\mathbf{v}$  is approached through a stream function  $\psi(r, \theta)$  defined by

$$v_r = -\frac{1}{r^2 \sin \theta} \frac{\partial \psi}{\partial \theta}, \quad v_\theta = \frac{1}{r \sin \theta} \frac{\partial \psi}{\partial r}.$$

After taking the curl of Eq. (3a) and using the fact that  $\mu$  and  $\beta$  only depend on  $r$  (because they are functions of  $\rho$ ), we have

$$\begin{aligned} \mu E^4(\psi) + \frac{d\mu}{dr} \frac{\partial}{\partial r} [E^2(\psi)] \\ - \lambda^{-2} \left[ \beta E^2(\psi) - \frac{d\beta}{dr} \frac{\partial \psi}{\partial r} \right] = 0, \end{aligned} \quad (9)$$

where

$$E^2 = \frac{\partial^2}{\partial r^2} + \frac{\sin \theta}{r^2} \frac{\partial}{\partial \theta} \left( \frac{1}{\sin \theta} \frac{\partial}{\partial \theta} \right). \quad (10)$$

Boundary conditions (8) become

$$r = 1: \quad \psi = \frac{\partial \psi}{\partial r} = 0, \quad (11a)$$

$$r \rightarrow \infty: \quad \psi \rightarrow \frac{1}{2} r^2 \sin^2 \theta. \quad (11b)$$

In dimensional terms, the drag force is<sup>19</sup>

$$\mathbf{F}_f = 8\pi\mu_s R \mathbf{U} \lim_{r \rightarrow \infty} \left[ \frac{\psi - \frac{1}{2} r^2 \sin^2 \theta}{r \sin^2 \theta} \right]. \quad (12)$$

By combining Eqs. (7) and (12) we can find  $L_h$ .

Equation (9) poses a singular perturbation problem when  $\lambda \ll 1$ . Since  $\beta = 0$  and  $\mu = 1$  to at least order  $\lambda^2$  when  $y$  is replaced by  $r$ , Eq. (9) simplifies considerably at distances such that  $r - 1 \gg \lambda$ . In this "outer region" we write the solution as

$$\psi^{(0)} = [\frac{1}{2} r^2 + Cr^{-1} + Dr] \sin^2 \theta, \quad (13)$$

$$C = C_0 + \lambda C_1 + \lambda^2 C_2 + \dots, \quad (14a)$$

$$D = D_0 + \lambda D_1 + \lambda^2 D_2 + \dots, \quad (14b)$$

where the  $C_n$  and  $D_n$  are constants. These constants are obtained below by matching  $\psi^{(0)}$  with the solution to Eq. (9) which is valid within the polymer layer. By combining Eqs. (7), (12), (13), and (14) we obtain the two parameters of Eq. (5):

$$A = -\frac{4}{3} D_1, \quad B = D_2 / D_1. \quad (15)$$

Within the inner region, where  $r - 1 \sim O(\lambda)$ , we replace  $r$  by the variable  $y = \lambda^{-1}(r - 1)$ . A solution to Eq. (9) is sought in the form

$$\psi^{(i)} = [F_0(y) + \lambda F_1(y) + \lambda^2 F_2(y) + \dots] \sin^2 \theta, \quad (16)$$

$$y = 0: \quad F_n = \frac{dF_n}{dy} = 0.$$

Substituting this expression into Eq. (9) and collecting terms of equal order in  $\lambda$  produces equations which must be solved for  $F_n(y)$ . The unknown boundary conditions on  $F_n$  at  $y \rightarrow \infty$  and the constants  $C_n$  and  $D_n$  are found by matching Eq. (13) with Eq. (16) at equivalent orders in  $\lambda$ :

$$\lim_{y \rightarrow \infty} \psi^{(i)} = [\psi^{(0)}]_{r=1+\lambda y}. \quad (17)$$

After performing this matching we find  $F_0 = F_1 = 0$  and the following:

$$\begin{aligned} D_0 = -\frac{3}{4}, \quad D_1 = \frac{1}{2} \lim_{y \rightarrow \infty} \left[ \frac{dF_2}{dy} - \frac{3}{2} y \right], \\ D_2 = \frac{1}{2} \lim_{y \rightarrow \infty} \left[ F_2 + \frac{dF_3}{dy} \right], \end{aligned} \quad (18)$$

$$\frac{d}{dy} \left[ \mu \frac{d^2 F_2}{dy^2} \right] - \beta \frac{dF_2}{dy} = 0, \quad (19)$$

$$y = 0: \quad F_2 = \frac{dF_2}{dy} = 0,$$

$$y \rightarrow \infty: \quad \frac{d^2 F_2}{dy^2} \rightarrow \frac{3}{2},$$

$$\frac{d}{dy} \left[ \mu \frac{d^2 F_3}{dy^2} \right] - \beta \frac{dF_3}{dy} = 2 \frac{d\mu}{dy} \frac{dF_2}{dy} - \frac{3}{2}, \quad (20)$$

$$y = 0: \quad F_3 = \frac{dF_3}{dy} = 0,$$

$$y \rightarrow \infty: \quad \frac{d^2 F_3}{dy^2} \rightarrow -\frac{3}{2} y - 2D_1.$$

In general, Eqs. (19) and (20) must be solved numerically given the dependence of  $\mu$  and  $\beta$  on  $\rho$ , and  $\rho$  on  $y$ . For this purpose, and to facilitate comparison between these re-

sults and those of the other flow configurations, we define new variables:

$$G = -\frac{2}{3} \frac{dF_2}{dy}, \quad H_t = -\frac{2}{3} \frac{dF_3}{dy}. \quad (21)$$

Equations (19) and (20) become

$$\frac{d}{dy} \left[ \mu \frac{dG}{dy} \right] - \beta G = 0, \quad (22)$$

$$y = 0: \quad G = 0,$$

$$y \rightarrow \infty: \quad \frac{dG}{dy} \rightarrow -1,$$

$$\frac{d}{dy} \left[ \mu \frac{dH_t}{dy} \right] - \beta H_t = 1 + 2G \frac{d\mu}{dy}, \quad (23)$$

$$y = 0: \quad H_t = 0,$$

$$y \rightarrow \infty: \quad \frac{dH_t}{dy} \rightarrow y - A.$$

The two parameters of Eq. (5) are obtained from Eqs. (15) and (18):

$$A = \lim_{y \rightarrow \infty} [G + y] \quad (24a)$$

$$B = A^{-1} \left[ \lim_{y \rightarrow \infty} \left( H_t - \frac{y^2}{2} + Ay \right) + \int_0^\infty (G + y - A) dy \right]. \quad (24b)$$

Thus, solutions of Eqs. (22) and (23) are needed to calculate  $A$  and  $B$  from Eq. (24). The only inputs needed are the polymer segment density profile  $\rho(y)$ , and the dependence of  $\mu$  and  $\beta$  on  $\rho$ .

## B. Rotation of a particle

The torque produced by the fluid on a particle without adsorbed polymer which rotates at angular velocity  $\Omega$  is

$$\mathbf{T}_f^{(0)} = -8\pi\mu_s R^3 \Omega \quad (\text{no polymer}). \quad (25)$$

The hydrodynamic thickness of an adsorbed polymer layer is defined as the increase in radius of the particle needed to account for the extra torque:

$$\mathbf{T}_f = -8\pi\mu_s (R + L_h)^3 \Omega \quad (\text{adsorbed polymer}). \quad (26)$$

$\mathbf{T}_f$  must be determined from solution of the modified Stokes equations so that  $L_h$  can be computed from Eq. (26).

Since inertial terms are assumed negligible, we can choose a coordinate system which rotates with the particle without adding apparent accelerations in the momentum equation. In this rotating coordinate system  $\mathbf{v}^{(p)} = 0$ . Equation (3) must be solved subject to the following boundary conditions:

$$r = 1: \quad \mathbf{v} = 0, \quad (27a)$$

$$r \rightarrow \infty: \quad \mathbf{v} \rightarrow -\mathbf{k} \times \mathbf{r}, \quad (27b)$$

where  $\mathbf{k}$  is the unit vector in the direction of  $\Omega$ .

As before the fluid is divided into outer ( $r - 1 \gg \lambda$ ) and inner [ $r - 1 \sim O(\lambda)$ ] regions. Since  $\mu \rightarrow 1$  and  $\beta$  decay exponentially to zero in the  $y$  variable, the form of Eq. (3) in the outer region has  $\mu = 1$  and  $\beta = 0$  to all orders in  $\lambda$ . The solution to Eq. (3) under these circumstances can be written as

$$p^{(0)} = \text{const},$$

$$\mathbf{v}^{(0)} = [-r + Mr^{-2}] \sin \theta \mathbf{i}_\phi,$$

$$M = M_0 + \lambda M_1 + \lambda^2 M_2 + \dots, \quad (28)$$

where the  $M_n$  are constants and  $\mathbf{i}_\phi$  is the unit vector along changes in the azimuthal angle. The values of  $M_n$  determine the torque on the sphere:

$$\mathbf{T}_f = -8\pi\mu_s R^3 [M_0 + \lambda M_1 + \lambda^2 M_2 + \dots] \Omega. \quad (29)$$

Comparing this expression with Eq. (26) we see that the parameters of Eq. (5) are

$$A = \frac{M_1}{3}, \quad B = \frac{M_2}{M_1} - \frac{M_1}{3}. \quad (30)$$

Within the inner region we look for a solution of the form

$$p^{(i)} = \text{constant},$$

$$\mathbf{v}^{(i)} = [F_0(y) + \lambda F_1(y) + \lambda^2 F_2(y) + \dots] \sin \theta \mathbf{i}_\phi,$$

$$y = 0: \quad F_n = 0. \quad (31)$$

Differential equations for  $F_n$  are obtained by substituting Eq. (31) into Eq. (3) and collecting terms of equivalent order in  $\lambda$ . The far-field conditions on  $F_n$  and the values of  $M_n$  are determined by asymptotically matching the inner and outer solutions for the velocity fields. The results to  $O(\lambda^2)$  are

$$M_0 = 1, \quad M_1 = 3 \lim_{y \rightarrow \infty} [G + y],$$

$$M_2 = 6 \lim_{y \rightarrow \infty} \left[ H - \frac{y^2}{2} + \frac{M_1}{3} y \right], \quad (32)$$

$$\frac{d}{dy} \left[ \mu \frac{dG}{dy} \right] - \beta G = 0, \quad (33)$$

$$y = 0: \quad G = 0,$$

$$y \rightarrow \infty: \quad \frac{dG}{dy} \rightarrow -1,$$

$$\frac{d}{dy} \left[ \mu \frac{dH_r}{dy} \right] - \beta H_r = -\mu \frac{dG}{dy} + \frac{G}{2} \frac{d\mu}{dy}, \quad (34)$$

$$y = 0: \quad H_r = 0,$$

$$y \rightarrow \infty: \quad \frac{dH_r}{dy} \rightarrow y - A,$$

where  $G = F_1/3$  and  $H_r = F_2/6$ . The parameters of Eq. (5) are obtained from Eqs. (30) and (32):

$$A = \lim_{y \rightarrow \infty} [G + y], \quad (35a)$$

$$B = A^{-1} \left[ 2 \lim_{y \rightarrow \infty} \left( H_r - \frac{y^2}{2} + Ay \right) - A^2 \right]. \quad (35b)$$

Note that Eq. (33) and (22) are identical, so that  $A$  is the same for translation and rotation of a particle. The  $B$  parameter appears to differ, however, when Eqs. (34) and (35b) are compared with Eqs. (23) and (24b).

## C. Intrinsic viscosity of a suspension of particles

In order to calculate the contribution made by suspended particles to the viscosity of a suspension, we must determine the velocity disturbance caused by each particle when

it is in a pure straining motion.<sup>20</sup> The undisturbed fluid velocity is

$$\mathbf{v}^{(00)} = \mathbf{E} \cdot \mathbf{r}, \quad (36)$$

where  $\mathbf{E}$  is a constant, symmetric tensor with zero trace. By adding the contributions of each particle to viscous forces on distant boundaries, neglecting interactions between the particles, one has Einstein's result for the intrinsic viscosity (based on number concentration of particles):

$$[\mu]^{(0)} = 2.5 \left( \frac{4}{3} \pi R^3 \right) \quad (\text{no polymer}). \quad (37)$$

When polymer is adsorbed equally to all particles, the intrinsic viscosity should increase. By defining  $L_h$  as the apparent increase in particle size, we have

$$[\mu] = 2.5 \left[ \frac{4}{3} \pi (R + L_h)^3 \right] \quad (\text{adsorbed polymer}). \quad (38)$$

This expression provides the basis for computing  $L_h$ .

Because  $\mathbf{v}^{(00)}$  is a pure straining motion, a particle with its center at  $\mathbf{r} = \mathbf{0}$  does not translate or rotate and hence  $\mathbf{v}^{(p)} = \mathbf{0}$ . Equation (3) must be solved subject to

$$r = 1: \quad \mathbf{v} = \mathbf{0}, \quad (39a)$$

$$r \rightarrow \infty: \quad \mathbf{v} \rightarrow \mathbf{E} \cdot \mathbf{r}, \quad (39b)$$

A further constraint is that the force exerted by the fluid on the particle is zero. Lamb's general solution<sup>19</sup> gives the following as a possible solution satisfying Eq. (39b) and the zero force condition:

$$p^{(0)} = Lr^{-5} \mathbf{E} : \mathbf{r} \mathbf{r}, \quad (40a)$$

$$\mathbf{v}^{(0)} = \left[ \frac{1}{2} Lr^{-5} - \frac{5}{2} Qr^{-7} \right] \mathbf{E} : \mathbf{r} \mathbf{r} \mathbf{r} + [1 + Qr^{-5}] \mathbf{E} \cdot \mathbf{r}, \quad (40b)$$

$$L = L_0 + \lambda L_1 + \lambda^2 L_2 + \cdots,$$

$$Q = Q_0 + \lambda Q_1 + \lambda^2 Q_2 + \cdots,$$

where the  $L_n$  and  $Q_n$  are constants to be determined by matching  $\mathbf{v}^{(0)}$  with the inner velocity field. Using the analysis of Batchelor<sup>20</sup> we have

$$[\mu] = -\frac{L}{2} \left( \frac{4}{3} \pi R^3 \right). \quad (41)$$

Comparing Eq. (38) with Eq. (41) gives

$$A = -\frac{L_1}{15}, \quad B = \frac{L_1}{15} + \frac{L_2}{L_1}. \quad (42)$$

For the inner region the solution has the form

$$p^{(i)} = [P_0(y) + \lambda P_1(y) + \lambda^2 P_2(y) + \cdots] \mathbf{E} : \mathbf{n} \mathbf{n}, \quad (43a)$$

$$\mathbf{v}^{(i)} = [F_0(y) + \lambda F_1(y) + \cdots] \mathbf{E} : \mathbf{n} \mathbf{n} \mathbf{n} + [S_0(y) + \lambda S_1(y) + \cdots] \mathbf{E} \cdot \mathbf{n}, \quad (43b)$$

$$y = 0: \quad F_n = 0, \quad S_n = 0,$$

where  $\mathbf{n} = r^{-1} \mathbf{r}$ . The far-field conditions on  $P_n$ ,  $F_n$ , and  $S_n$  are determined by matching Eq. (43) into Eq. (40). Differential equations for these functions are obtained by substituting Eq. (43) into Eq. (3) and collecting expressions of equivalent order in  $\lambda$ . The components of Eq. (3a) which are proportional to  $\mathbf{n}$  yield equations which are solved for  $S_n$ ; Eq. (3b) can be directly integrated to obtain  $F_n$  from  $S_n$ . The functions  $P_n$  are determined from the terms of Eq. (3a) proportional to  $\mathbf{n} \mathbf{n} \mathbf{n}$ . The results of matching inner and outer fields are

$$L_0 = 5Q_0 = -5, \quad L_1 = 3Q_1 = 3 \lim_{y \rightarrow \infty} [S_1 - 5y],$$

$$Q_2 = \lim_{y \rightarrow \infty} [S_2 + 4Q_1 y - 10Q_0 y^2],$$

$$L_2 = 5Q_2 + 2 \lim_{y \rightarrow \infty} [F_2 - 7Q_1 y + \frac{35}{2} Q_0 y^2]. \quad (44)$$

With  $G$  defined as  $-S_1/5$  and  $H_v$  as  $-S_2/20$ , the Stokes equations gives

$$\frac{d}{dy} \left[ \mu \frac{dG}{dy} \right] - \beta G = 0, \quad (45)$$

$$y = 0: \quad G = 0,$$

$$y \rightarrow \infty: \quad \frac{dG}{dy} \rightarrow -1,$$

$$\frac{d}{dy} \left[ \mu \frac{dH_v}{dy} \right] - \beta H_v = \frac{1}{2} - \frac{1}{2} \mu \frac{dG}{dy} + \frac{1}{4} G \frac{d\mu}{dy}, \quad (46)$$

$$y = 0: \quad H_v = 0,$$

$$y \rightarrow \infty: \quad \frac{dH_v}{dy} \rightarrow y - A.$$

The solution for  $F_2$  is found by integrating Eq. (3b):

$$F_2 = 20H_v - 15 \int_0^y G(\hat{y}) d\hat{y}. \quad (47)$$

Finally, the parameters of Eq. (5) are obtained from Eqs. (42) and (44):

$$A = \lim_{y \rightarrow \infty} [G + y], \quad (48a)$$

$$B = -A + 2A^{-1} \left[ 2 \lim_{y \rightarrow \infty} \left( H_v - \frac{y^2}{2} + Ay \right) + \int_0^\infty (G + y - A) dy \right]. \quad (48b)$$

Note that  $A$  here is identical to that for translation and rotation of a particle.

### III. EVALUATION OF THE HYDRODYNAMIC PARAMETERS $A$ AND $B$

The result for very thin double layers  $A$  is the same for all three dynamical cases. The function  $G(y)$  is first obtained by solving Eq. (22) and  $A$  is then computed from Eq. (24a). The only properties of the polymer layer that are required are  $\mu$  and  $\beta$ , both of which must be related to the segment distribution  $\rho(y)$  by an appropriate hydrodynamic model. The correction for particle curvature  $B$  differs among the three flow situations. One must first solve Eqs. (23), (34), or (46) for  $H(y)$  and substitute the result into Eqs. (24b), (35b), or (48b) to determine  $B$  for particle translation, rotation, or the intrinsic viscosity of a suspension.

Unless otherwise stated, we assume  $\mu = 1$  throughout the polymer layer. Under this condition we can use the results of the previous section to show the following is correct for any dependence of  $\beta$  on  $y$ :

$$B_r = 0, \quad (49a)$$

$$B_v = 2B_t, \quad (49b)$$

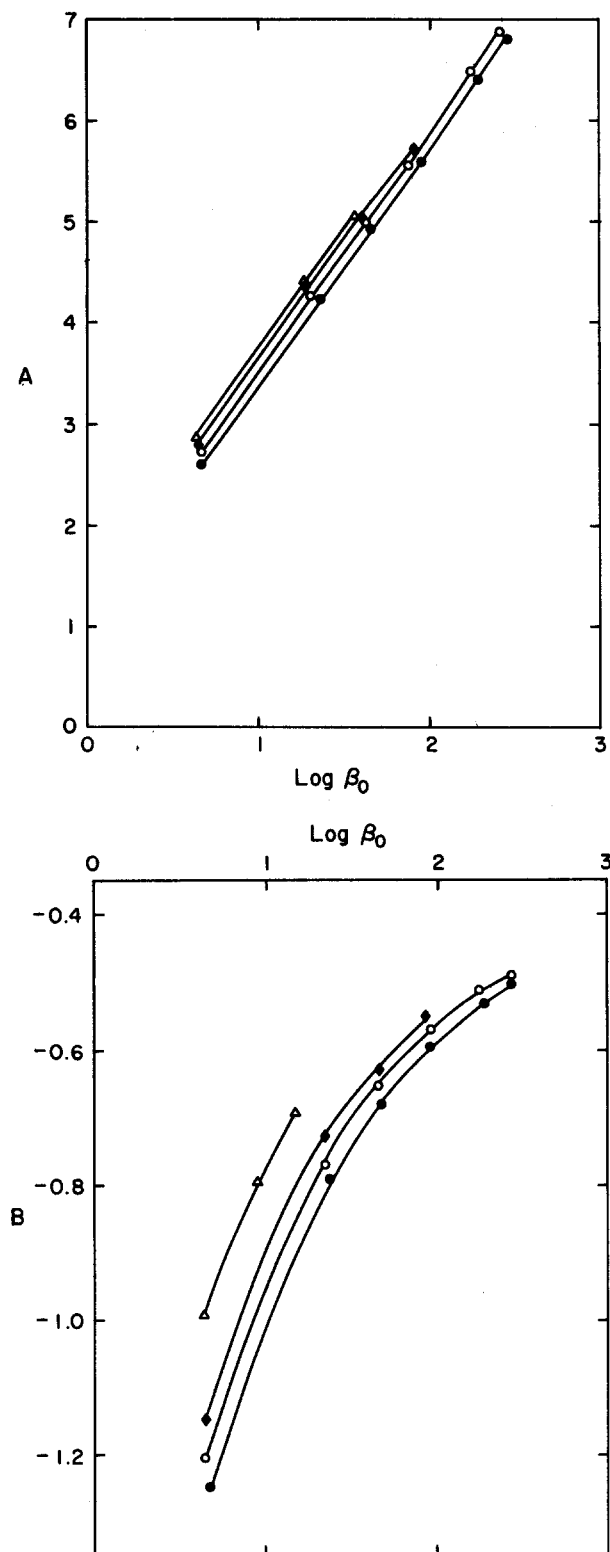


FIG. 2. Calculations for no tails ( $\eta = 0$ ). In the non-free-draining cases, Eq. (55) was used for  $f$ . Solid curves here and in subsequent figures represent interpolation between calculated points. free-draining  $\bullet$ , non-free-draining  $\circ$  ( $\delta/a = 10$ ),  $\blacklozenge$  ( $\delta/a = 5$ ), and  $\triangle$  ( $\delta/a = 2$ ).

where the subscripts  $r$ ,  $v$ , and  $t$  refer to rotation, intrinsic viscosity (pure straining flow), and translation. Therefore, we need solve only Eq. (22) to obtain  $A$ , which is the same for all three flow situations, and Eq. (23) to obtain  $B_t$ . In the

ensuing calculations we assume a polymer segment density of the form

$$\rho(y) = \rho_0[e^{-y} + \eta e^{-\alpha y}] \quad (50)$$

to account for two exponentially decaying distributions. We imagine the primary distribution ( $\rho_0 e^{-y}$ ) to represent segments in the loops and the secondary distribution to represent the tails.  $\alpha$  is the ratio of loop-to-tail length scales and should be less than one. The length scale ( $\delta$ ) used to normalize  $y$  is that of the loops. The total number of polymer segments in the loops per area of particle surface equals  $\delta \rho_0$ ; the corresponding number in the tails is  $\alpha^{-1} \eta \delta \rho_0$ , and hence the fraction of segments contained in the tails is  $\eta/(\alpha + \eta)$ .

In calculating  $A$  and  $B_t$ , we use Eqs. (4) and (50) to determine  $\beta(y)$ :

$$\beta = \beta_0[e^{-y} + \eta e^{-\alpha y}] f, \quad (51a)$$

$$\beta_0 \equiv \frac{\delta^2 \zeta}{\mu_s} \rho_0 = \frac{9}{2} \left( \frac{\delta}{a} \right)^2 \phi_0, \quad (51b)$$

where  $a$  is the Stokes radius of each segment, given by Eq. (2), and  $\phi_0$  is the volume fraction based on  $\rho_0$  (total segment density at the interface) assuming the segments are hard spheres of radius  $a$ . Note that the shielding parameter ( $b/l$ ) used by Varoqui and Dejaridin<sup>18</sup> is related to our parameters by

$$b/l = \left( \frac{2}{9\phi_0} \right)^{-1/2} \left( \frac{\delta}{a} \right). \quad (52)$$

Our feeling is that for Eq. (3) to be a realistic model of flow through the polymer chains,  $\delta/a \gg 1$ ; assuming  $\phi_0$  is of order 0.1, we expect typical values of  $\beta_0$  to be in the range  $10^1$ – $10^3$ , which gives a shielding parameter consistent with the range explored by Varoqui and Dejaridin.<sup>18</sup>

We first consider systems with *no tails* ( $\eta = 0$ ). In the free-draining limit ( $f = 1$ ) an analytical solution to Eq. (22) can be found if  $y$  is replaced by a new variable equal to  $2\beta_0^{1/2} \exp(-y/2)$ . Substituting the solution for  $G$  into Eq. (24a) gives

$$A = \ln \beta_0 + 2\gamma + 2 \frac{K_0(2\beta_0^{1/2})}{I_0(2\beta_0^{1/2})} \\ \doteq \ln \beta_0 + 2\gamma \quad \text{if } \beta_0 > 4, \quad (53)$$

where  $I_0$  and  $K_0$  are modified Bessel functions and  $\gamma$  is Euler's constant (0.5772). This result was previously derived by deGennes<sup>9</sup> for flow through porous media. With the same variable transformation we have obtained an analytical solution to Eq. (23), which gives the following when substituted into Eq. (24b) and requiring  $\beta_0 > 4$ :

$$B_t \doteq A - 8A^{-1} \int_0^{2\beta_0^{1/2}} x^{-1} [K_0(x) + \ln(x/2) + \gamma] dx \\ = A - 8A^{-1} \left\{ \int_0^4 x^{-1} [K_0(x) + \ln(x/2) + \gamma] dx \right. \\ \left. - 0.8002 + \frac{1}{2} [\ln(2\beta_0^{1/2})]^2 \right. \\ \left. - (\ln 2 - \gamma) \ln(2\beta_0^{1/2}) \right\}. \quad (54)$$

Figure 2 shows plots of Eqs. (53) and (54).

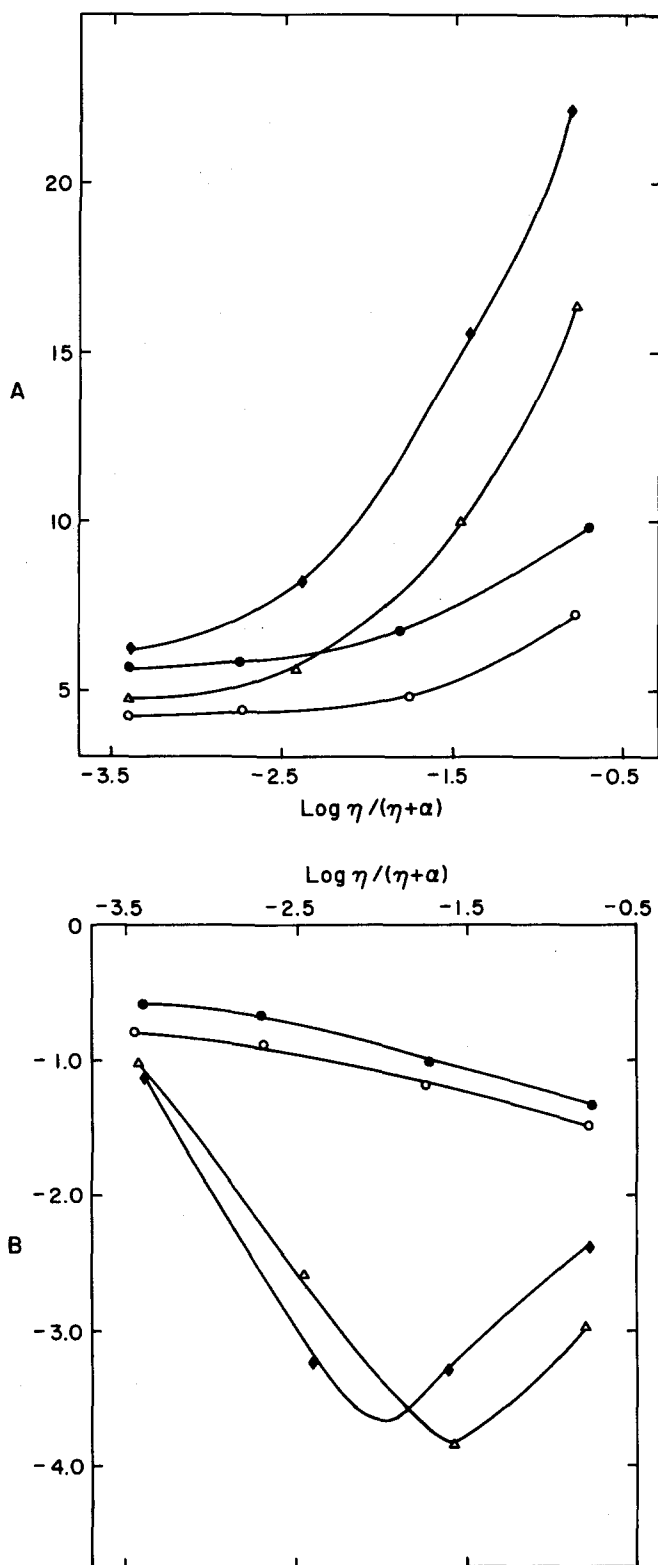


FIG. 3. Calculations of parameters as a function of the fraction of segments contained in the tails. Free-draining limit ( $f=1$ ) assumed.  $\beta_0 = 100$ ,  $\blacklozenge$  ( $\alpha = 0.25$ ),  $\bullet$  ( $\alpha = 0.5$ ).  $\beta_0 = 25$ ,  $\triangle$  ( $\alpha = 0.25$ ),  $\circ$  ( $\alpha = 0.5$ ).

We have numerically solved Eqs. (22) and (23) for the case of hydrodynamic interactions among the polymer segments. The expression we used for  $f(\phi)$ , where  $\phi = (4/3)\pi a^3 \rho(y)$ , is a combination of a modified Brinkman

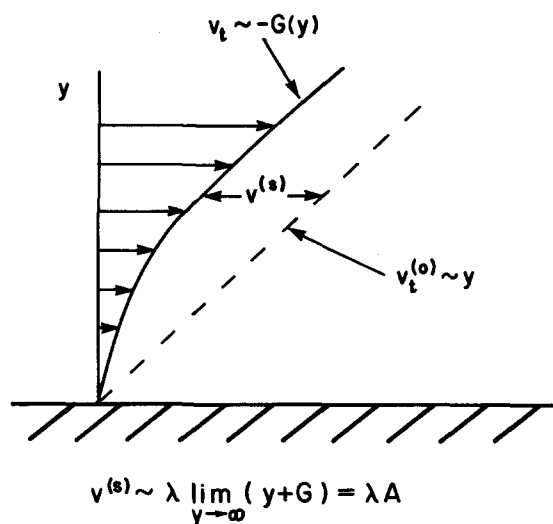


FIG. 4. Slip velocity at outer edge of the polymer layer in the limit  $\lambda \rightarrow 0$ .

equation<sup>16</sup> at low  $\phi$  and the Blake-Kozeny equation at high  $\phi$ <sup>17</sup>:

$$f = 1 + 2.121\phi^{1/2} + 0.84\phi \ln \phi + 16.456\phi \quad \text{for } \phi < 0.29, \\ = \frac{8.34\phi}{(1-\phi)^3} \quad \text{for } \phi > 0.29. \quad (55)$$

The resulting values of  $A$  and  $B_t$ , assuming no tails ( $\eta = 0$ ), are plotted in Fig. 2 for several values of  $\delta/a$ . The differences between these calculations and the free-draining results are rather small; the reason for this is discussed later.

We next consider the effect of tails by solving for  $G$  and  $H_t$  in the free-draining limit over a range of  $\eta$  and  $\alpha$ . In Fig. 3  $A$  and  $B_t$  are plotted vs the fraction of polymer segments contained in the tails. It is clear that a small number of tails can exert a large effect on  $L_h$  if  $\alpha$  is sufficiently small. These results support the contention by Cohen Stuart *et al.*<sup>4</sup> that the tails cannot generally be neglected in determining the hydrodynamic effects of adsorbed polymers.

We have also performed calculations which include polymer effects on viscosity. An expression for  $\mu$  vs local polymer segment density was obtained by using an empirical expression for the shear viscosity of a suspension of rigid spheres as a function of volume fraction.<sup>21</sup> In no case where these viscous effects significant to either  $A$  or  $B_t$ , and we conclude that one can safely ignore local effects of the polymer on apparent viscosity.

#### IV. THIN POLYMER LAYERS AND NONUNIFORM POLYMER ADSORPTION

In the limit of very thin polymer layers ( $\lambda \rightarrow 0$ ) the local description of flow within the polymer layer is well approximated as flow past a flat plate. Let  $v_t(y)$  represent the fluid velocity parallel to the particle surface; the normal component of velocity is  $O(\lambda)$  relative to  $v_t$ . In the absence of polymer  $v_t^0 \sim y$ , while  $v_t \sim -G(y)$  when the polymer is present. The difference in velocity caused by the polymer is therefore proportional to  $(G+y)$  and approaches a limiting value equal to  $A$  as  $y \rightarrow \infty$ , as shown in Fig. 4. This velocity difference, called a "slip velocity," appears to be a discontinuity in



$\mathbf{v}$  when viewed from the outer region on the length scale of particle radius. Such apparent velocity discontinuities appear in the description of various phoretic transport phenomena such as electrophoresis.<sup>22</sup> It seems that deGennes (see Ref. 18) recognized this slip velocity as the source of the polymer effect on flow through porous media.

For a sphere undergoing translation ( $\mathbf{U}$ ) and rotation ( $\boldsymbol{\Omega}$ ), the slip velocity (in dimensional form) is

$$\mathbf{v}^{(s)} \equiv \lim_{r \rightarrow R^+} [\mathbf{v} - \mathbf{U} - R \boldsymbol{\Omega} \times \mathbf{n}] = A\lambda \left[ \frac{3}{2}(\mathbf{I} - \mathbf{nn}) \cdot \mathbf{U} + 3R \boldsymbol{\Omega} \times \mathbf{n} \right]. \quad (56)$$

This expression is correct at any point on the particle (just outside the polymer layer) in the asymptotic limit  $\lambda \rightarrow 0$ , even if  $A$  is a function of position ( $\theta, \phi$ ) on the surface, as long as the length scale of  $\nabla A$  is  $O(R)$  rather than  $O(\delta)$ . Variations in  $A$  over the surface of a single particle could result, say, from uneven adsorption of polymer. The value of  $A$  at any point on the surface is calculated from Eqs. (22) and (24a), with  $\beta$  and  $\mu$  determined by the polymer properties at that point.

The slip velocity can be used with Lamb's general solution of the Stokes equations<sup>19</sup> to directly compute the force and torque experienced by a translating, rotating sphere. Some details of the analysis are given in the Appendix. The following results are exact in the limit  $\lambda \rightarrow 0$ :

$$\mathbf{F}_f = -6\pi\mu_s R [\mathbf{I} + \lambda \langle A \rangle \mathbf{I} + \mathbf{P}_2] \cdot \mathbf{U} + 18\pi\mu_s R^2 \lambda \mathbf{P}_1 \times \boldsymbol{\Omega}, \quad (57a)$$

$$\mathbf{T}_f = -8\pi\mu_s R^3 [\mathbf{I} + 3\lambda \langle A \rangle \mathbf{I} - 2\mathbf{P}_2] \cdot \boldsymbol{\Omega} - 18\pi\mu_s R^2 \lambda \mathbf{P}_1 \times \mathbf{U}, \quad (57b)$$

where the brackets  $\langle \rangle$  denote an average over the surface of the particle, and  $\mathbf{P}_1$  and  $\mathbf{P}_2$  are the dipole and quadrupole moments of  $A$  [see Eqs. (A15) and (A16)]. The dipole produces an  $O(\lambda)$  coupling between translation and rotation, while the force-velocity and torque-angular velocity relationships depend on both the average value of  $A$  and the quadrupole moment. If  $A$  is constant over the surface then there is no translation-rotation coupling, and  $L_h = A\delta$  for both translational and rotational motions as derived earlier.

As a simple example of how a nonuniform layer of polymer can affect the dynamics, consider the case where polymer is uniformly adsorbed to one hemispherical surface ( $A = A_0$ ) but no polymer is present on the other hemisphere ( $A = 0$ ). Let  $\mathbf{e}$  be the unit vector describing the orientation of the polymer-adsorbed hemisphere. From Eq. (57) we have

$$\mathbf{F}_f = -6\pi\mu_s R (1 + \frac{1}{2} A_0 \lambda) \mathbf{U} + \frac{3}{2} \pi\mu_s R^2 A_0 \lambda \mathbf{e} \times \boldsymbol{\Omega}, \quad (58a)$$

$$\mathbf{T}_f = -8\pi\mu_s R^3 (1 + \frac{3}{2} A_0 \lambda) \boldsymbol{\Omega} - \frac{3}{2} \pi\mu_s R^2 A_0 \lambda \mathbf{e} \times \mathbf{U}. \quad (58b)$$

Considering only effects to  $O(\lambda)$ , the force is independent of the orientation if  $\mathbf{T}_f = 0$ . However, there is still rotation of the particle due to the translation-rotation coupling:

$$(\mathbf{T}_f = 0) \quad \boldsymbol{\Omega} = -\frac{9}{16} \frac{A_0 \delta}{R^2} \mathbf{e} \times \mathbf{U}. \quad (59)$$

This rotation tends to align the particle such that the axis of the dipole is parallel to  $\mathbf{U}$  (with the polymer-coated side directed downstream) while rotational Brownian motion tends to randomize the orientation of  $\mathbf{e}$ . The rotational Peclet number ( $Pe_r$ ) equals  $|\boldsymbol{\Omega}|/D_r$ , where  $D_r$  is the rotational diffusion coefficient; for the present example,

$$Pe_r = \left( \frac{9\pi}{2} \frac{\mu_s}{kT} A_0 \delta R \right) U \sin \theta, \quad (60)$$

where  $\theta$  is the solid angle between  $\mathbf{e}$  and  $\mathbf{U}$ . The steady-state orientational probability of  $\mathbf{e}$  is more or less restricted to those angles  $180^\circ > \theta > \theta^*$ , where  $\theta^*$  is the orientation for which  $Pe_r = 1$ . Given  $R = 1 \mu\text{m}$ ,  $\delta = 0.05 \mu\text{m}$ ,  $A_0 = 5$ , and  $U = 100 \mu\text{m/s}$  in a fluid having  $\mu_s = 10^{-2} \text{ gm/cm} \cdot \text{s}$  at  $25^\circ$ ,  $\theta^* = 179.3$  which means that there is essentially total alignment of  $-\mathbf{e}$  with the direction of flow. The characteristic time for reaching this steady-state condition from an initial arbitrary orientation is  $R^2/(A_0 \delta U) \approx 40$  ms. This example demonstrates that a dipole in polymer adsorption can cause alignment of a particle when it moves in response to an applied force.

## V. DISCUSSION

There are four main results of the theory developed here. First, we have derived simple equations which must be solved, given a polymer segment distribution  $\rho(y)$  and rheological parameters ( $\mu, \beta$ ), to determine the parameters  $A$  and  $B$  of Eq. (5). The theory is correct to  $O(\lambda)$ , thereby allowing a correction for surface curvature when calculating  $L_h$ . Second, we proved that  $A$  is the same for all three flow configurations of Fig. 1. While this result is assumed in the literature, our work offers the first proof of this assertion. Third, if polymer effects on  $\mu$  in the adsorbed layer are negligible, a good assumption based on our numerical calculations, then  $B = 0$  for rotation and  $B_v = 2B_t$ , where the subscripts  $v$  and  $t$  denote intrinsic viscosity and translation, respectively. Finally, we derived expressions [Eq. (57)] for the fluid force and torque on a translating, rotating particle which could have a *nonuniform* coating of polymer on its surface; these expressions apply to the limit  $\lambda \rightarrow 0$ .

As mentioned above, our numerical calculations indicate that it is usually safe to neglect the polymer effect on  $\mu$  and simply set  $\mu = 1$  in all equations. If we further assume free-draining flow ( $f = 1$ ) and neglect any tails ( $\eta = 0$ ),  $A$  and  $B_t$  are given by Eqs. (53) and (54). Considering the  $\lambda \rightarrow 0$  limit and the parameters in  $\beta_0$ , we use the result for  $A$  to write

$$L_h \sim \delta (\ln \delta + \ln \Gamma + \text{constant}),$$

where  $\Gamma$  is the amount of polymer adsorbed per area of particle surface. Although a theory for the adsorption of polymer is required to relate  $\delta$  to  $\Gamma$  as well as properties of the polymer, it is still clear that  $L_h$  is not simply proportional to  $\delta$  or  $\Gamma$ .

Figure 2 shows that hydrodynamic interactions [ $f$  given by Eq. (55)] among polymer segments produce relatively small effects on  $A$  and  $B_t$ , especially when  $\delta/a \gtrsim 5$ . This can be understood by considering flow within a polymer layer in the limit  $\lambda \rightarrow 0$ ; the tangential component of velocity is proportional to  $G$ :

$$v_i \sim -G(y). \quad (61)$$

The solution to Eq. (22) in the case of free-draining segments and no tails is

$$G = 2 \left[ \frac{K_0(2\beta_0^{1/2})}{I_0(2\beta_0^{1/2})} I_0(2\beta^{1/2}) - K_0(2\beta^{1/2}) \right] \\ \doteq -2K_0(2\beta^{1/2}) \quad \text{if } \beta_0 \gg 1, \quad \beta_0 \gg \beta, \quad (62)$$

where  $\beta$  is given by Eq. (51a) with  $f = 1$  and  $\eta = 0$ . If  $\beta > 4$  then  $v_i < 0.02$  and the precise value of  $\beta$  is unimportant since  $v_i$  is essentially zero. This means the value of  $f$  is only important when  $\beta < 4$ ; using Eq. (51) we define a critical volume fraction of polymer segments as

$$\phi_{\text{crit}} = \frac{8}{9} \left( \frac{a}{\delta} \right)^2 \frac{1}{f}, \quad (63)$$

such that  $f$  need only be used for  $\phi(y) < \phi_{\text{crit}}$ . If  $\delta/a = 5$  then Eq. (55) gives  $\phi_{\text{crit}} = 0.022$  and  $f(\phi_{\text{crit}}) = 1.6$ , so that even though  $f$  could be as high as 20 or 30 near the particle surface, hydrodynamic interactions are only significant when  $f < 1.6$  and thus may be neglected. Similar arguments apply to explain why polymer contributions to  $\mu$  may be neglected. Figure 2 shows that as  $\delta/a$  is made smaller, hydrodynamic interactions make a greater contribution to both  $A$  and  $B$ .

Our conclusion that a free-draining model for flow through an adsorbed polymer leads to a good approximation for  $A$ , at least when  $\delta/a \gtrsim 5$ , seems to contradict Cohen Stuart *et al.*<sup>4</sup> who stress the importance of hydrodynamic interactions among polymer segments. The reason for this disagreement is found in their parameter  $C_H$ , which in our nomenclature is defined by

$$C_H = \frac{\mu_s \phi(y)}{4\xi a^2 \rho(y)}. \quad (64)$$

[Note also that they assumed  $f = (1 - \phi)^{-1}$ , compared to Eq. (55) here.] When Stokes law is used to relate  $\xi$  to segment size we obtain  $C_H = 1/18$ . Cohen Stuart *et al.* arbitrarily chose  $C_H \approx 1$  instead, which would cause Eq. (63) to be replaced by

$$\phi_{\text{crit}} = 16 \left( \frac{a}{\delta} \right)^2 \frac{1}{f}. \quad (65)$$

In this case hydrodynamic interactions would be important in the calculation of  $A$  even if  $\delta/a = 5$  because  $\phi < \phi_{\text{crit}}$  throughout the entire adsorbed layer. In effect Cohen Stuart *et al.* used two size parameters for the segment dimension, one for the lattice dimension that relates  $\phi$  to  $\rho$ , and another for the "Stokeslet" size (based on  $\xi$ ) of each segment, with the Stokeslet radius being 1/18 that on which  $\phi$  is based. In our calculations only one segment dimension ( $a$ ) is used.

The calculations plotted in Fig. 3 support arguments in the literature<sup>4</sup> that the adsorbed polymer tails can contribute significantly to  $L_h$  even if they represent a small fraction of the segments compared to the loops. The reason for this apparent disproportionate effect of the tails is that their length scale exceeds the mean length of the loops,<sup>12</sup> i.e.,  $\alpha < 1$ . To illustrate the importance that a small number of tails can have, consider the case  $\alpha = 0.25$  of Fig. 3; the tails are making a substantial contribution to  $A$  even though the fraction of the polymer segments that are in the tails is only 0.3%.

In computing the  $B$  parameter we have assumed a sim-

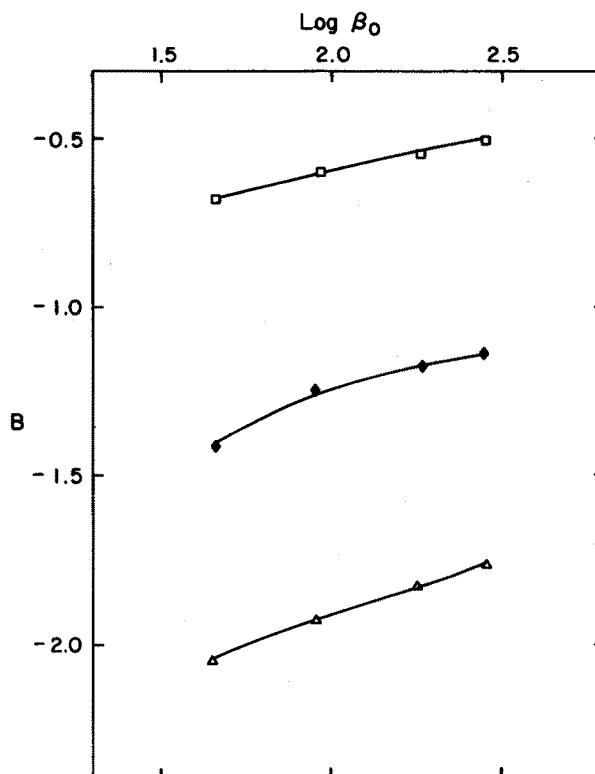


FIG. 5. Effect of  $b$  [see Eq. (66)] on the curvature correction. Free-draining limit ( $f = 1$ ) assumed.  $\square$  ( $b = 0$ ),  $\blacklozenge$  ( $b = 0.5$ ), and  $\triangle$  ( $b = 1$ ).

ple exponential decay of the polymer segment density. This could be an oversimplification since the convex nature of the particle's surface might reduce excluded volume effects among the polymer segments. A segment density of the following form allows for curvature effects on polymer distribution:

$$\rho = \rho_0 \frac{e^{-y}}{1 + b\lambda y}. \quad (66)$$

In the free-draining limit,  $\beta(y)$  has the form of Eq. (66) with  $\rho_0$  replaced by  $\beta_0$ . The equations that must be solved for  $H(y)$  are altered; for example, Eq. (23) would be modified to

$$\frac{d}{dy} \left( \mu \frac{dH_i}{dy} \right) - \beta_0 e^{-y} H_i = 1 + 2G \frac{d\mu}{dy} - b\beta_0 y e^{-y} G \quad (67)$$

with the same boundary conditions as for Eq. (23). We have numerically solved Eq. (67) with  $\mu = 1$  and substituted the results into Eq. (24b) to compute  $B_i$ . These calculations, which are plotted in Fig. 5, show that positive values of  $b$  enhance the curvature effect as one would expect.

As a final point, we consider the effect of segment distribution on  $L_h$  when  $\delta$  and  $\Gamma$  are held constant. The free-draining model is used with  $\mu = 1$ . If  $\rho(y)$  is given by Eq. (1) then  $A$  is calculated from Eq. (53). Now consider a segment distribution that is uniform over the distance  $\delta$ :

$$\rho = \rho_0 \quad \text{if } 0 < y < \delta, \\ = 0 \quad \text{if } \delta < y. \quad (68)$$

Substitution of this profile into Eqs. (22) and (24a) gives

$$A = 1 - \beta_0^{-1/2} \tanh \beta_0^{1/2}. \quad (69)$$

Comparison of this result with Eq. (53) shows that  $L_h$  is about six times greater (if  $\beta_0 \approx 10^2$ ) for an exponential distribution of segments than for the same amount of polymer uniformly distributed over a region of thickness  $\delta$ .

In summary, we have developed a fluid dynamical description of how a thin layer of an adsorbed polymer affects the dynamics of a single particle in three different flow fields. We have purposely avoided restricting the analysis to a specific theory for polymer adsorption; on the contrary, the value of our results is that they allow for a general form for the polymer segment distribution to be substituted into the equations from which the hydrodynamic thickness of the polymer is calculated. Different types of adsorbed structures (e.g., loops and tails) are allowed, and one could even account for a molecular weight distribution of the polymer if a theory for its adsorption were known. The restrictions of our theory are (1) the particle must be spherical; (2)  $\lambda$  must be small, but not necessarily zero as in other theories; and (3) flow within the polymer layer must be described by Eq. (3) with  $\mu$  and  $\beta$  known functions of the local polymer segment density.

## ACKNOWLEDGMENTS

This work was supported by the National Science Foundation (CBT-8412332). J. O. Kim was supported by N. I. H. Training Grant GM-07477 and by a Rockwell Graduate Fellowship. We appreciate the numerous discussions with Professor M. Jhon.

## APPENDIX: FORCE AND TORQUE ON A SPHERE WITH A NONUNIFORM LAYER OF POLYMER

The sphere translates at  $\mathbf{U}$  and rotates at  $\mathbf{\Omega}$ . The asymptotic limit  $\lambda \rightarrow 0$  is considered here. In this limit the flow within the adsorbed polymer layer is one dimensional. The flow outside the polymer layer is described by the conventional Stokes equations with the following boundary conditions:

$$r \rightarrow R^+: \quad \mathbf{v} = \mathbf{U} + R \mathbf{\Omega} \times \mathbf{n} + \mathbf{v}^{(s)}, \quad (A1)$$

$$r \rightarrow \infty: \quad \mathbf{v} \rightarrow 0. \quad (A2)$$

(Note that in this section dimensional variables are used.) The slip velocity  $\mathbf{v}^{(s)}$  is the change in fluid velocity at the outer edge of the polymer layer ( $y \rightarrow \infty$ ) caused by the polymer segments. Its value is determined by the sum of the effects for translation and rotation:

$$\mathbf{v}^{(s)} = A\lambda \left[ \frac{3}{2}(\mathbf{I} - \mathbf{nn}) \cdot \mathbf{U} + 3R \mathbf{\Omega} \times \mathbf{n} \right], \quad (A3)$$

where  $A$  is the parameter defined by Eq. (24a). Now we allow  $A$  to be a function of position ( $\theta, \phi$ ) on the sphere's surface, as long as the length scale of  $\nabla A$  is  $O(R)$  and hence much greater than the layer thickness [ $O(\delta)$ ].

The force ( $\mathbf{F}_f$ ) and torque ( $\mathbf{T}_f$ ) exerted by the surrounding fluid on the particle plus adsorbed polymer can be obtained directly from Lamb's general solution of Stokes flow<sup>19,22</sup>:

$$\mathbf{F}_f = 2\pi\mu_s R [3\alpha_1 + \beta_1], \quad (A4)$$

$$\mathbf{T}_f = 4\pi\mu_s R^2 \gamma_1. \quad (A5)$$

The constant vectors ( $\alpha_1, \beta_1, \gamma_1$ ) are computed from the velocity field at the outer edge of the polymer layer ( $r \rightarrow R^+$ ):

$$\alpha_1 = -\mathbf{U} - 3\langle \mathbf{nn} \cdot \mathbf{v}^{(s)} \rangle, \quad (A6)$$

$$\beta_1 = 3R \langle (\nabla \cdot \mathbf{v}^{(s)}) \mathbf{n} \rangle, \quad (A7)$$

$$\gamma_1 = -2R \mathbf{\Omega} - 3R \langle \mathbf{nn} \cdot (\nabla \times \mathbf{v}^{(s)}) \rangle, \quad (A8)$$

$$\langle f \rangle \equiv (4\pi)^{-1} \int \int_{r=R^+} f \sin \theta d\theta d\phi.$$

The force-velocity relationship can be cast into the form

$$\mathbf{F}_f = -\mu_s [\mathbf{K}^{(T)} \cdot \mathbf{U} + \mathbf{C}^{(TR)} \cdot \mathbf{\Omega}], \quad (A9)$$

$$\mathbf{T}_f = -\mu_s [\mathbf{C}^{(RT)} \cdot \mathbf{U} + \mathbf{K}^{(R)} \cdot \mathbf{\Omega}]. \quad (A10)$$

The resistance coefficients ( $\mathbf{K}^{(T)}, \mathbf{K}^{(R)}, \mathbf{C}^{(TR)}, \mathbf{C}^{(RT)}$ ) are constants which depend on the size of the particle and the hydrodynamic effect of the polymer layer. These coefficients are obtained by combining Eqs. (A3)–(A8), allowing for  $A$  being a function of position.

$$\mathbf{K}^{(T)} = 6\pi R [\mathbf{I} + 3\lambda \langle A \mathbf{nn} \rangle],$$

$$\begin{aligned} \mathbf{K}^{(R)} &= 8\pi R^3 [\mathbf{I} + 9\lambda (\langle A \mathbf{nn} \rangle - \frac{1}{2} R \langle \mathbf{n} \nabla A \rangle)], \\ \mathbf{C}^{(TR)} &= -\mathbf{C}^{(RT)} = -18\pi R^3 \lambda \langle \mathbf{nn} \times \nabla A \rangle. \end{aligned} \quad (A11)$$

It can be shown that the coupling coefficient  $\mathbf{C}^{(TR)}$  is anti-symmetric.

The above relations can be put into a simpler form by using the following identities, which are proven by expanding  $A$  in terms of surface harmonics.

$$\langle A \mathbf{nn} \rangle = \frac{1}{3} [\langle A \rangle \mathbf{I} + \mathbf{P}_2], \quad (A12)$$

$$R \langle \mathbf{n} \nabla A \rangle = \mathbf{P}_2, \quad (A13)$$

$$R \langle \mathbf{nn} \times \nabla A \rangle = \mathbf{I} \times \mathbf{P}_1. \quad (A14)$$

$\langle A \rangle$  is the surface average of  $A$ , while  $\mathbf{P}_1$  and  $\mathbf{P}_2$  are the dipole and quadrupole moments:

$$\mathbf{P}_1 = \langle \mathbf{n} A \rangle, \quad (A15)$$

$$\mathbf{P}_2 = \langle (3\mathbf{nn} - \mathbf{I}) A \rangle. \quad (A16)$$

Using these expressions in Eqs. (A9)–(A11) we have

$$\begin{aligned} \mathbf{F}_f &= -6\pi\mu_s R [\mathbf{I} + \lambda (\langle A \rangle \mathbf{I} + \mathbf{P}_2)] \cdot \mathbf{U} \\ &\quad + 18\pi\mu_s R^2 \lambda \mathbf{P}_1 \times \mathbf{\Omega}, \end{aligned} \quad (A17)$$

$$\begin{aligned} \mathbf{T}_f &= -8\pi\mu_s R^3 [\mathbf{I} + 3\lambda (\langle A \rangle \mathbf{I} - 2\mathbf{P}_2)] \cdot \mathbf{\Omega} \\ &\quad - 18\pi\mu_s R^2 \lambda \mathbf{P}_1 \times \mathbf{U}. \end{aligned} \quad (A18)$$

## NOMENCLATURE

- $a$  = Stokes radius of polymer segment, Eq. (2) (cm).
- $A$  = parameter defined by Eq. (5).
- $B$  = parameter defined by Eq. (5).
- $f$  = hydrodynamic interaction parameter, Eq. (4).
- $\mathbf{F}_f$  = force exerted by the fluid on the particle (dyn).
- $G$  = function defined by Eq. (22).
- $H$  = function defined by Eqs. (23), (34), or (46).
- $k$  = Boltzmann constant (erg/K).
- $L_h$  = equivalent hydrodynamic thickness of polymer layer defined by Eqs. (7), (26), or (38) (cm).
- $\mathbf{n}$  = unit normal vector on the particle's surface.

$p$  = pressure (made nondimensional by  $\mu_s V^*/R$ ).  
 $P_1$  = dipole moment of  $A$ , Eq. (A15).  
 $P_2$  = quadrupole moment of  $A$ , Eq. (A16).  
 $\mathbf{r}$  = position vector from center of particle (made nondimensional by  $R$ ).  
 $R$  = particle radius (cm).  
 $T$  = temperature (K).  
 $\mathbf{T}_f$  = torque exerted by the fluid on the particle (dyn cm).  
 $\mathbf{U}$  = translational velocity of a particle (cm/s).  
 $\mathbf{v}$  = fluid velocity (sometimes made nondimensional by  $V^*$ ).  
 $V^*$  = characteristic velocity (cm/s).  
 $y = \lambda^{-1}(r - 1)$ .  
 $\alpha = \delta_{\text{loop}}/\delta_{\text{tail}}$ .  
 $\beta$  = function defined by Eq. (4).  
 $\beta_0$  = parameter defined by Eq. (51b).  
 $\Gamma$  = polymer adsorbed per surface area of particle (segments  $\text{cm}^{-2}$ ).  
 $\delta$  = length scale of segment distribution (cm), equal to  $\delta_{\text{loop}}$  if both loops and tails present.  
 $\zeta$  = Stokes friction coefficient of a polymer segment ( $\text{g s}^{-1}$ ).  
 $\eta$  = fraction of tails as defined by Eq. (49).  
 $\lambda = \delta/R$ .  
 $\mu_s$  = fluid viscosity ( $\text{g/cm s}$ ).  
 $\mu$  = viscosity inside polymer layer (made nondimensional by  $\mu_s$ ).  
 $[\mu]$  = intrinsic viscosity ( $\text{cm}^3/\text{particle}$ ).

$\rho$  = polymer segment distribution (segments  $\text{cm}^{-3}$ ).  
 $\phi = (4/3)\pi a^3 \rho$ .  
 $\Omega$  = angular velocity of a particle ( $\text{s}^{-1}$ ).

- <sup>1</sup>D. P. Yavorsky, Ph.D. thesis, University of Pennsylvania, 1981.
- <sup>2</sup>E. Pefferkorn, P. Dejardin, and R. Varoqui, *J. Colloid Interface Sci.* **63**, 353 (1978).
- <sup>3</sup>M. J. Garvey, Th. F. Tadros, and B. Vincent, *J. Colloid Interface Sci.* **55**, 440 (1975).
- <sup>4</sup>M. A. Cohen Stuart, F. H. W. H. Wajen, T. Cosgrove, B. Vincent, and T. L. Crowley, *Macromolecules* **17**, 1825 (1984).
- <sup>5</sup>C. A. J. Hoeve, *J. Chem. Phys.* **42**, 2558 (1965); **43**, 3007 (1965).
- <sup>6</sup>C. A. J. Hoeve, *J. Polym. Sci. C* **30**, 361 (1970); **34**, 1 (1971).
- <sup>7</sup>A. Silberberg, *J. Phys. Chem.* **66**, 382 (1962).
- <sup>8</sup>A. Silberberg, *J. Chem. Phys.* **48**, 2835 (1968).
- <sup>9</sup>P. G. deGennes, *Rep. Prog. Phys.* **32**, 187 (1969).
- <sup>10</sup>P. G. deGennes, *Macromolecules* **13**, 1069 (1980).
- <sup>11</sup>R. J. Roe, *J. Chem. Phys.* **60**, 4192 (1974).
- <sup>12</sup>J. M. H. M. Scheutjens and G. J. Fleer, *J. Phys. Chem.* **83**, 1619 (1979).
- <sup>13</sup>J. M. H. M. Scheutjens and G. J. Fleer, *J. Phys. Chem.* **84**, 178 (1980).
- <sup>14</sup>J. M. H. M. Scheutjens and G. J. Fleer, *Adv. Colloid Interface Sci.* **16**, 341 (1982).
- <sup>15</sup>T. Cosgrove, B. Vincent, T. L. Crowley, and M. A. Cohen Stuart, in *Polymer Adsorption and Dispersion Stability*, ACS Symp. Ser. 240, edited by E. D. Goddard and B. Vincent (American Chemical Society, Washington, D. C., 1984), pp. 147-202.
- <sup>16</sup>S. Kim and W. B. Russell, *J. Fluid Mech.* **154**, 269 (1985).
- <sup>17</sup>R. B. Bird, W. E. Stewart, and E. N. Lightfoot, *Transport Phenomena* (Wiley, New York, 1960).
- <sup>18</sup>R. Varoqui and P. Dejardin, *J. Chem. Phys.* **66**, 4395 (1977).
- <sup>19</sup>J. Happel and H. Brenner, *Low Reynolds Number Hydrodynamics* (Noordhoff, Groningen, 1973).
- <sup>20</sup>G. K. Batchelor, *J. Fluid Mech.* **41**, 545 (1970).
- <sup>21</sup>D. J. Jeffrey and A. Acrivos, *Amer. Inst. Chem. Engrs. J.* **22**, 417 (1976).
- <sup>22</sup>J. L. Anderson, *J. Colloid Interface Sci.* **105**, 45 (1985).